

Preparation and Characterization of Lithium Niobate Single Crystals Doped with 4.02–5.38 mol % Zn

I. V. Biryukova^a, S. M. Masloboeva^a*, I. N. Efremov^a, N. A. Teplyakova^a, and M. N. Palatnikov^a

^a *Tananaev Institute of Chemistry and Technology of Rare Elements and Mineral Raw Materials (separate subdivision), Kola Scientific Center (Federal Research Center), Russian Academy of Sciences, Apatity, Murmansk oblast, 184209 Russia*

**e-mail: sofia_masloboeva@mail.ru*

Received June 29, 2022; revised December 21, 2022; accepted December 26, 2022

Abstract—Using homogeneous doping, a Nb_2O_5 :4.5 mol % Zn precursor, and lithium carbonate, we have synthesized a single-phase LiNbO_3 :4.1 mol % Zn growth charge, which was then used to grow lithium niobate crystals by the Czochralski technique. High-speed optical quality evaluation results for the crystals and their calculated piezoelectric modulus d_{333} demonstrate that they have high optical quality. Photoinduced light scattering and laser conoscopy characterization results for homogeneously and directly doped crystals containing 4.02–5.38 mol % Zn confirm their high optical homogeneity and laser damage resistance. The crystals have absolutely no photorefractive response. Our results can be used in the growth of large LiNbO_3 :Zn crystals with a small coercive field, which are of interest for making laser light converters based on periodically poled structures.

Keywords: lithium niobate single crystals, doping, microdefects, static piezoelectric modulus, photoinduced light scattering, laser conoscopy

DOI: 10.1134/S0020168523020048

INTRODUCTION

LiNbO_3 :M (Mg, Zn, In, Sc, and others) doped lithium niobate single crystals have been the subject of intense research for many years now [1–7] and are regarded as optical materials widely used in nonlinear, integrated, and polarization optics, as well as in laser engineering and optoelectronics. However, despite the recent advances in their technology, the preparation of optically homogeneous single crystals remains a topical issue. Results obtained by researchers are sometimes contradictory. One of the main causes of this is that, in most studies, LiNbO_3 :M crystals were investigated with no allowance for their prior history: specific features of growth charge components, the growth charge synthesis method, the way in which the single crystals were doped, physicochemical features of the melt, and growth conditions. The effect of melt structure on the properties of lithium niobate crystals was studied in greatest detail by Uda and Tiller [8] and Kimura et al. [9]. Not only did they present theoretical calculations of the equilibrium coefficient of molten lithium niobate with a dopant, but they also experimentally determined the electromotive force using the micro-pulling-down method, which made it possible to find an optimal composition for growth of chemically homogeneous defect-free LiNbO_3 :Mg single crystals [9]. In most other reports, at best only some growth process parameters were specified. The effect of the doping procedure on the structure and proper-

ties of LiNbO_3 :Mg crystals was examined by Palatnikov et al. [10], who demonstrated that LiNbO_3 :Mg crystals identical in dopant concentration but grown under different conditions differed markedly in properties. In studies of LiNbO_3 :Zn single crystals by Palatnikov et al. [11–13], varying the doping level in small steps allowed three dopant concentration ranges between which the properties of the crystals changed sharply to be located with sufficiently high accuracy: from 4.02 to 5.38 (first), from 5.38 to 6.8 (second), and from 6.8 to 9.0 mol % Zn (third).

The objectives of this work were to grow LiNbO_3 :Zn single crystals from a growth charge synthesized via homogeneous doping (HD) using a Nb_2O_5 :Zn precursor with Zn concentration lying in the first concentration range; to study their single-domain state, photorefractive properties, and structural and optical homogeneity; and compare them with directly doped crystals.

EXPERIMENTAL

Nb_2O_5 :Zn niobium pentoxide containing 4.5 mol % Zn was prepared according to a technological scheme described by Masloboeva et al. [14]. The Zn dopant was introduced via sorption of zinc ions into high-purity niobium hydroxide while it was mixed with a nitric acid solution of $\text{Zn}(\text{NO}_3)_2$ (extrapure grade) with a predetermined concentration. After filtration

and washing, the hydroxide precipitate was dried and calcined at 1000°C for 3 h.

For LiNbO₃:Zn (HD) crystal growth, a zinc-doped granulated growth charge of congruent composition ($[\text{Li}_2\text{O}]/[\text{Nb}_2\text{O}_5] = 0.946$) was prepared by a synthesis/granulation process using a mixture of Li₂CO₃ (extrapure grade) and Nb₂O₅:Zn as a precursor. The required amount of Li₂CO₃ was calculated for pure Nb₂O₅. After mechanical activation of the starting materials for 24 h in a tumbling drum, the mixture was placed in a platinum crucible and slightly compacted. It was heat-treated in a PVK-1.4-25 annealing furnace. Below 1100°C, the heating rate was 200°C/h. After holding for 3 h, the mixture was heated to 1243°C at a rate of 100°C/h and then held there for 5 h.

LiNbO₃:Zn (HD) crystals 40 mm in diameter, with a 40-mm-long cylindrical body, were grown in air in the [001] direction by Czochralski pulling from platinum crucibles 75 mm in inner diameter. We used induction-heated growth units equipped with an automatic crystal diameter control system. The translation speed was 1.1 mm/h, and the rotation rate was 14 rpm. The axial temperature gradient was ~1°C/mm. The total charge weight in the crucible was 1150 g, and no more than 25% of the melt was used for crystal growth.

To relieve the thermoelastic stress, the crystals were heat-treated at 1200°C for 24 h. The Nb²O⁵:Zn precursor, LiNbO₃:Zn growth charge, and grown crystals were analyzed for zinc by atomic emission spectroscopy (Shimadzu ICPS-9000 spectrometer). The error of determination by this method was estimated at ~2%. The phase composition of the growth charge and solidified residual melt was determined by X-ray diffraction on a Shimadzu XRD-6100 X-ray diffractometer. The phases present were identified using the JCPDS-ICDD database (release 2002).

The LiNbO₃:Zn (HD) crystals were converted to a single-domain state via high-temperature electrodiffusion annealing (HTEDA) in a dc poling field during cooling of the samples at a rate of 20°C/h in the temperature range from 1241 to 888°C.

The degree of conversion of the LiNbO₃:Zn crystals to a single-domain state was evaluated by measuring the static d_{333} piezoelectric modulus of a crystalline boule using a procedure described by Masloboeva et al. [15]. The optical quality of the material was assessed from the average number of scattering centers per unit volume of the crystals under study.

The laser damage resistance and optical homogeneity of the single crystals were assessed using photoinduced light scattering (PILS) and laser conoscopy—methods described in detail elsewhere [16–19].

RESULTS AND DISCUSSION

To grow LiNbO₃:Zn (HD) crystals in the first dopant concentration range, we synthesized a growth

charge containing 4.1 mol % Zn. According to chemical analysis data, the percentages of niobium and lithium in the growth charge (62.3 and 4.36 wt %, respectively) corresponded to the congruent melting composition. The individual contents of cation trace impurities in the growth charge, determined on a DFS-13 spectrograph, were Pb, Ni, Cr, Co, V, Ti, Fe, Al, $<2 \times 10^{-4}$; Ca, Si, $<1 \times 10^{-3}$; and Ta, $<1 \times 10^{-2}$ wt %, which allowed it to be classified as “high-purity.” According to X-ray diffraction results, the growth charge was single-phase.

The synthesized growth charge was used to grow two single crystals by the Czochralski technique: from growth charges containing 4.10 mol % Zn (crystal 1) and 4.15 mol % Zn (crystal 2). To prepare crystal 2, the starting growth charge was added to the solidified residual melt after the growth of crystal 1.

The experimental data processing results for the grown LiNbO₃:Zn (HD) crystals (Table 1) demonstrated that the zinc concentration varied very little in the growth direction: the difference in dopant concentration between their cone and tail end was near the accuracy of the method used to determine zinc concentration (± 0.1 mol %). Such a dopant distribution attests to a high chemical homogeneity of the crystals, characteristic of growth conditions with $K_{\text{eff}} = 1$, whereas the single crystals under investigation have a distribution coefficient $K_{\text{eff}} < 1$. A uniform dopant distribution over LiNbO₃:Zn crystals is observed as well in melt–crystal–dopant systems in the case of direct doping (DD) [12], where a ZnO oxide dopant is added to a growth charge before melting in a crucible (Table 1, crystals 3, 4). At the same time, K_{eff} is larger in the case of LiNbO₃:Zn (HD) single crystals. We find that the use of a homogeneously doped growth charge with zinc concentrations near the first concentration threshold makes it possible to obtain crystals containing ~10% more zinc. It seems likely that HD of lithium niobate crystals leads to a qualitatively different melt structure, which results in smaller dopant distribution coefficients throughout the concentration range studied.

X-ray diffraction results for the solidified residual melt after the growth of crystals 1 and 2 (HD) showed that they were grown from single-phase melts, consisting of LiNbO₃ [20] (card no. 88-0289). At the same time, X-ray diffraction characterization of the tail end of crystals 3 and 4 (DD) indicated the presence of two phases, LiNbO₃ and Li₃NbO₄ (card no. 75-0902), suggesting that a part of the crystalline boules should be rejected.

High-speed evaluation of the optical quality of the LiNbO₃:Zn (HD) samples showed that they were absolutely free of extended defects and scattering centers, demonstrating high optical purity of the material.

Figure 1 shows plots of polarization charge (Q_p) against applied force (F) for the crystals before and after conversion to a single-domain state. We per-

Table 1. Zinc concentration in the melt (C_m), crystal cone (C_c), and tail end (C_t) and zinc distribution coefficient ($K_{\text{eff}} = C_c/C_m$) in crystals 1 (HD), 2 (HD), 3 (DD), and 4 (DD)

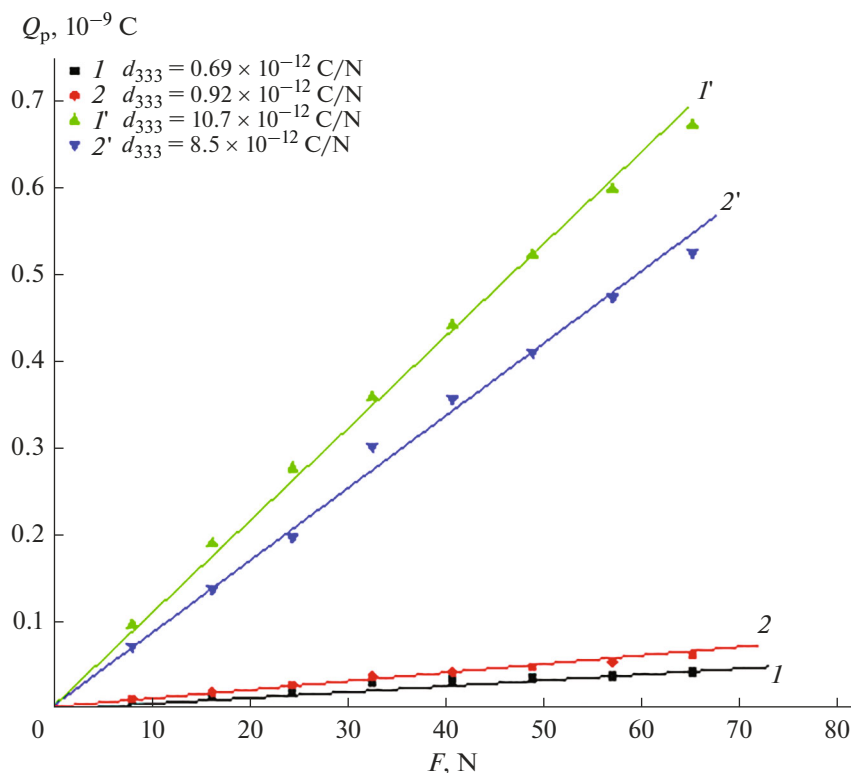
Crystal	C_m , mol %	C_c , mol %	C_t , mol %	$\Delta C = C_c - C_t$, mol %	K_{eff}
1	4.10	3.87	3.76	0.11	0.944
2	4.15	3.85	3.78	0.07	0.928
3	4.02	3.43	3.53	0.1	0.853
4	5.38	3.95	3.86	0.09	0.734

formed three series of measurements on the LiNbO_3 :Zn (HD) samples, short-circuiting them between the series for 1 h. In plotting the data, we used average values. It is seen from Fig. 1 that the as-grown crystals exhibited essentially no piezoelectric effect and that Q_p was only a weak linear function of F , with $d_{333} < 1$. HTEDA of the single crystals in a dc poling field during cooling of the samples at a rate of $20^\circ\text{C}/\text{h}$ in the temperature range from 1241 to 888°C gave rise to a well-defined piezoelectric effect (Fig. 1, plots 1', 2') due to stable unipolarity of the crystals under investigation.

We calculated the piezoelectric modulus d_{333} of each sample: $d_{333} = 10.7 \times 10^{-12}$ and 8.5×10^{-12} C/N for crystals 1 and 2, respectively. Despite the rather large piezoelectric modulus of the crystals, approach-

ing reference data ($d_{333} \geq 8 \times 10^{-12}$ C/N) [21], the plot of Q_p against F for crystal 2 (plot 2') shows a small jump in polarization charge Q_p and, accordingly a deviation from linearity. This suggests that the load-induced field influenced residual domains or unbalanced charges, probably left after conversion to a single-domain state. Crystal 1 had a larger piezoelectric modulus and a linear plot of Q_p against F .

In our PILS experiments (Fig. 2), the electric field vector E of the laser light was parallel to the polar axis Z of the crystal and the laser beam was directed along the X axis. Both crystals studied showed no photorefractive response, the PILS indicatrix did not open, and there was only circular scattering by static structural defects. The scattering pattern did not vary over time and its shape remained unchanged throughout the

**Fig. 1.** Plots of Q_p against F for crystals (1, 1') 1 and (2, 2') 2 (1, 2) before and (1', 2') after conversion to a single-domain state. Q_p is the polarization charge and F is the applied force.

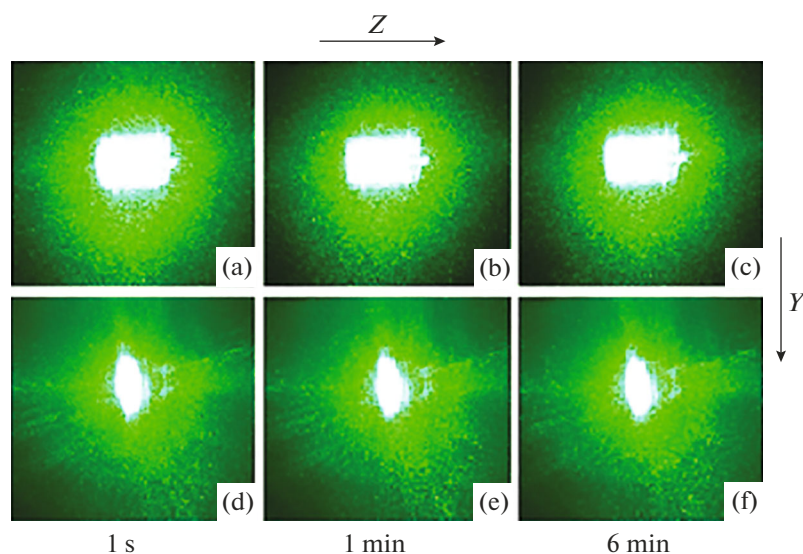


Fig. 2. Pils patterns of the $\text{LiNbO}_3\text{:Zn}$ crystals (a–c) 1 and (d–f) 2 ($\lambda = 532 \text{ nm}$, $P = 160 \text{ mW}$).

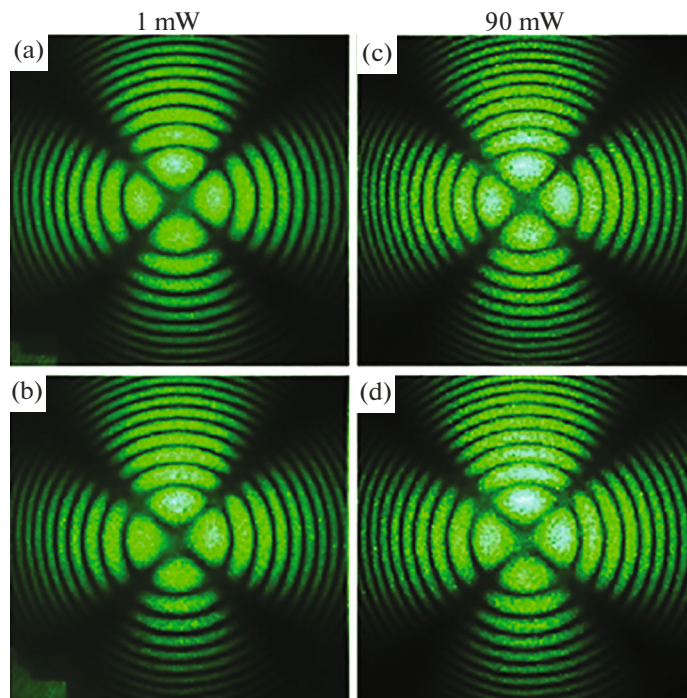


Fig. 3. Conoscopic patterns of crystal 1 (3-mm-thick plate, $\lambda = 532 \text{ nm}$, $P = 1$ and 90 mW).

experiment. At the same time, the Pils patterns of crystal 2 (Figs. 2d–2f) were slightly more blurred, pointing to a somewhat larger scattering power of this crystal compared to crystal 1, which was attributable to the lower degree of conversion of crystal 2 to a single-domain state.

We studied conoscopic patterns of the $\text{LiNbO}_3\text{:Zn}$ (HD) crystals 1 and 2 (Figs. 3, 4). The patterns obtained by scanning over the plane of the input face differ markedly (panels a and b against c and d). It is

seen from Figs. 3a, 3c, 4a, and 4c that the conoscopic patterns are almost perfect and correspond to those of a uniaxial crystal of good optical quality. The conoscopic patterns in Figs. 3b, 3d, 4b, and 4d have small signs of anomalous optical biaxiality, showing up as a slight elongation of the “Maltese cross” in the vertical direction from the center to the corresponding optical indicatrix distortion direction of the crystal, with no discontinuity in the center of the “Maltese cross.” Isochromes retain circular symmetry. The presence of

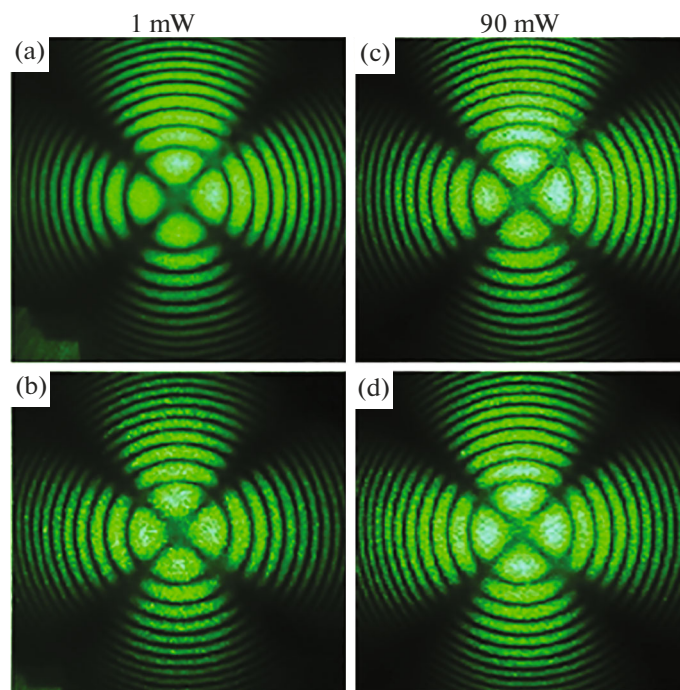


Fig. 4. Conoscopic patterns of crystal 2 (3-mm-thick plate, $\lambda = 532$ nm, $P = 1$ and 90 mW).

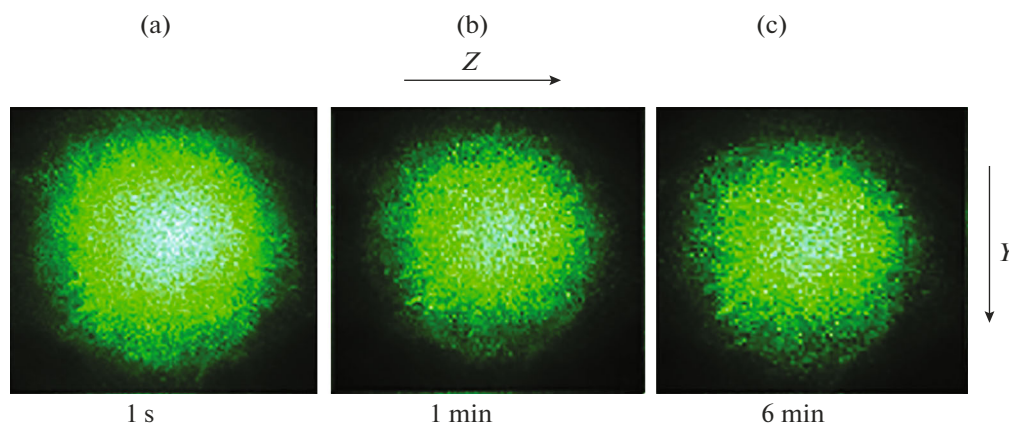


Fig. 5. PILS patterns of the $\text{LiNbO}_3\text{:Zn}$ (DD) crystal ($C_m = 5.38$ mol % Zn, 3-mm-thick plate, $\lambda = 532$ nm, $P = 160$ mW).

anomalous optical biaxiality in the conoscopic patterns may be due to nonuniform incorporation of the dopant into the structure of the crystals. Raising the laser output power to 90 mW caused no further distortion of the conoscopic pattern. Thus, the conoscopic patterns and PILS data for both crystals demonstrate that they have no photorefractive response and suggest that they have rather high optical homogeneity.

In addition, the $\text{LiNbO}_3\text{:Zn}$ (DD) crystal grown from a melt with $C_m = 5.38$ mol % Zn (crystal 4) was characterized by PILS measurements and conoscopy. The PILS and conoscopy results are presented in Figs. 5 and 6.

The crystal showed no photorefractive response, the PILS indicatrix did not open, and there was only circular scattering by static structural defects. The scattering pattern varied slightly during the first min-

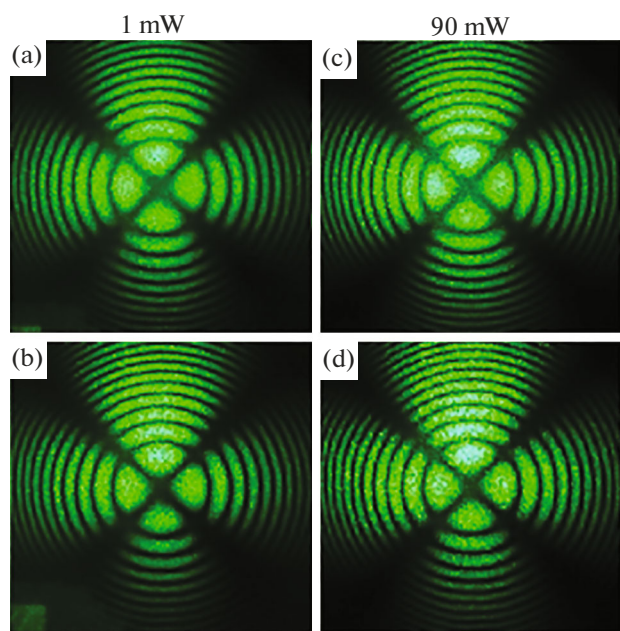


Fig. 6. Conoscopic patterns of the LiNbO₃:Zn (DD) crystal ($C_m = 5.38$ mol % Zn, 3-mm-thick plate, $\lambda = 532$ nm, $P = 1$ and 90 mW).

ute and then remained unchanged, retaining its shape for 6 min. It is worth noting that the PILS patterns had no central layer, corresponding to the cross section of the laser beam. This points to laser beam energy dissipation by structural defects in the crystal, which is also evidenced by the observed decrease in the scattering pattern diameter during the first minute.

Scanning over the plane of the input face of the crystal, we obtained slightly different conoscopic patterns (Figs. 6a and 6b against 6c and 6d). We observed slight bleaching in the top left of the “Maltese cross.” In the conoscopic patterns in Figs. 6b and 6d, the “Maltese cross” is slightly elongated in the vertical direction, corresponding to the optical indicatrix distortion direction of the crystal, with no discontinuity of the “Maltese cross.” Isochromes retain circular symmetry. Such distortion of the conoscopic patterns is associated with the small anomalous optical biaxiality of the crystal.

The present results demonstrate that the crystal has high optical homogeneity, comparable to that the LiNbO₃:Zn (HD) crystals 1 and 2.

CONCLUSIONS

Lithium niobate crystals have been grown from a LiNbO₃:4.1 mol % Zn growth charge synthesized via HD using a Nb₂O₅:4.5 mol % Zn precursor. It has been shown that, in the composition range 4.02–5.38 mol % Zn, the homogeneously doped crystals contain ~10% more zinc than do directly doped crystals and have a larger effective distribution coefficient.

LiNbO₃:Zn (HD) crystals grow from a single-phase melt and have no limitations on the fraction of the solidified melt at which a transparent single-crystal boule free of second-phase inclusions can be obtained.

High-speed optical quality evaluation results demonstrate that the crystals are absolutely free of microdefects and scattering centers. Their single-domain state has been confirmed by piezoelectric measurements. The d_{333} piezoelectric modulus of crystals 1 and 2 has been determined to be $d_{333} = 10.7 \times 10^{-12}$ and 8.5×10^{-12} C/N, respectively. The PILS and laser oscopy characterization results show that the LiNbO₃:Zn crystals have a high degree of optical homogeneity without a photorefractive response, suggesting that the material is laser damage resistant.

LiNbO₃:Zn crystals of similar quality can be grown via DD of a melt containing 4.02 or 5.38 mol % Zn, but their size (cylindrical body length) is limited because of the presence of second-phase inclusions. Therefore, which of the processes should be chosen for the growth of large LiNbO₃:Zn single crystals for commercial purposes will be determined by assessment of their cost effectiveness.

CONFLICT OF INTEREST

The authors declare that they have no conflicts of interest.

REFERENCES

1. Volk, T.R. and Rubinina, N.M., Nonphotorefractive impurities in lithium niobate: magnesium and zinc, *Fiz. Tverd. Tela* (Leningrad), 1991, vol. 33, no. 4, pp. 1192–1201.
2. Schlarb, U., Woehlecke, M., Gather, B., Reichert, A., Betzler, K., Volk, T., and Rubinina, N., Refractive indices of Zn-doped lithium niobate, *Opt. Mater.*, 1995, vol. 4, pp. 791–795. [https://doi.org/10.1016/0925-3467\(95\)00018-6](https://doi.org/10.1016/0925-3467(95)00018-6)
3. Chernaya, T.S., Volk, T.R., Verin, I.A., and Simonov, V.I., Threshold concentrations in zinc-doped lithium niobate crystals and their structural conditionality, *Crystallogr. Rep.*, 2008, vol. 53, no. 4, pp. 573–578.
4. Zhang, Y., Xu, Y.H., Li, M.H., and Zhao, Y.Q., Growth and properties of Zn doped lithium niobate crystal, *J. Cryst. Growth*, 2001, vol. 233, pp. 537–540. [https://doi.org/10.1016/S0022-0248\(01\)01614-1](https://doi.org/10.1016/S0022-0248(01)01614-1)
5. Abdi, F., Aillerie, M., Fontana, M., Bourson, P., Volk, T., Maximov, B., Sulyanov, S., Rubinina, N., and Wöhlecke, M., Influence of Zn doping on electrooptical properties and structure parameters of lithium niobate crystals, *Appl. Phys. B*, 1999, vol. 68, pp. 795–799. <https://doi.org/10.1007/s003400050706>
6. Zhao, L., Wang, X., Wang, B., Wen, W., and Zhang, T.Y., ZnO-doped LiNbO₃ single crystals studied by X-ray and density measurements, *Appl. Phys. B*, 2004, vol. 78, no. 6, pp. 769–774. <https://doi.org/10.1007/s00340-004-1503-9>
7. Aillerie, M., Bourson, P., Mostefa, M., Abdi, F., and Fontana, M.D., Photorefractive damage in congruent

- LiNbO₃: Part I. Zinc doped lithium niobate crystals, *J. Phys.: Conf. Ser.*, 2013, vol. 416, p. 012001. <http://iopscience.iop.org/1742-6596/416/1/012001>.
8. Uda, S. and Tiller, W.A., The dissociation and ionization of LiNbO₃ melts, *J. Cryst. Growth*, 1992, vol. 121, nos. 1–2, pp. 155–190. [https://doi.org/10.1016/0022-0248\(92\)90185-L](https://doi.org/10.1016/0022-0248(92)90185-L)
 9. Kimura, H., Koizumi, H., Uchidab, T., and Uda, S., Influence of impurity doping on the partitioning of intrinsic ionic species during the growth of LiNbO₃ crystal from the melt, *J. Cryst. Growth*, 2009, vol. 311, pp. 1553–1558. <https://doi.org/10.1016/J.JCRYSGRO.2008.09.178>
 10. Palatnikov, M.N., Biryukova, I.V., Masloboeva, S.M., Makarova, O.V., Kravchenko, O.E., Yanichev, A.A., and Sidorov, N.V., Structure and optical homogeneity of LiNbO₃:Mg? crystals grown from different charges, *Inorg. Mater.*, 2013, vol. 49, no. 7, pp. 715–720. <https://doi.org/10.1134/S0020168513060083>
 11. Palatnikov, M.N., Biryukova, I.V., Makarova, O.V., Sidorov, N.V., Efremov, V.V., Efremov, I.N., Teplyakova, N.A., and Manukovskaya, D.V., Research of concentration conditions for growth of strongly doped LiNbO₃:Zn single crystals, in *Advanced Materials: Manufacturing, Physics, Mechanics and Applications*, Cham: Springer Nature, 2016, vol. 175, pp. 87–99. https://doi.org/10.1007/978-3-319-26324-3_7
 12. Palatnikov, M.N., Sidorov, N.V., Makarova, O.V., and Biryukova, I.V., *Fundamental'nye aspekty tekhnologii sil'no legirovannykh kristallov niobata litiya* (Fundamental Aspects of the Technology of Heavily Doped Lithium Niobate Crystals), Apatity: Kol'sk. Nauchn. Tsentr Ross. Akad. Nauk, 2017.
 13. Palatnikov, M.N., Biryukova, I.V., Masloboeva, S.M., Makarova, O.V., Manukovskaya, D.V., and Sidorov, N.V., The search of homogeneity of LiNbO₃ crystals grown of charge with different genesis, *J. Cryst. Growth*, 2014, vol. 386, pp. 113–118. <https://doi.org/10.1016/j.jcrysgro.2013.09.038>
 14. Masloboeva, S.M., Kalinnikov, V.T., Zalkind, O.A., Kadyrova, G.I., and Kuznetsov, V.Ya., Preparation of Zn²⁺-doped niobium pentoxide for lithium niobate crystal growth, *Tsvetn. Met.*, 2012, no. 5, pp. 89–92.
 15. Masloboeva, S.M., Efremov, I.N., Biryukova, I.V., and Palatnikov, M.N., Growth and characterization of a boron-doped lithium niobate single crystal, *Inorg. Mater.*, 2020, vol. 56, no. 11, pp. 1147–1152. <https://doi.org/10.1134/S0020168520110072>
 16. Maksimenko, V.A., Syui, A.V., and Karpets, Yu.M., *Fotoindutsirovannyye protsessy v kristallakh niobata litiya* (Photoinduced Processes in Lithium Niobate Crystals), Moscow: Fizmatlit, 2008.
 17. Syui, A.V., Sidorov, N.V., and Antonycheva, E.A., *Fotorefraktivnyye svoystva i osobennosti stroeniya nelineino-opticheskogo kristalla niobata litiya* (Photorefractive Properties and Detailed Structure of Lithium Niobate Nonlinear Optical Crystals), Khabarovsk: DVGUPS, 2011.
 18. Pikoul, O.Y., Determination of optical sign of a crystal by conoscopy method, *J. Appl. Crystallogr.*, 2010, vol. 43, pp. 949–954. <https://doi.org/10.1107/S0021889810025161>
 19. Pikoul, O.Yu., Alekseeva, L.V., Povkh, I.V., Stroganov, V.I., Rudoi, K.A., Tolstov, E.V., and Krishtop, V.V., Distinctive features of an optical system for producing large conoscopic patterns, *Izv. Vyssh. Uchebn. Zaved., Pribo-rostr.*, 2004, vol. 47, no. 12, pp. 53–55.
 20. Hsu, R., Maslen, E.N., Boulay, D., and Ishizawa, N., Synchrotron X-ray studies of LiNbO₃ and LiTaO₃, *Acta Crystallogr., Sect. B: Struct. Sci.*, 1997, vol. 53, pp. 420–428. <https://doi.org/10.1107/S010876819600777X>
 21. Blistanov, A.A., Bondarenko, V.S., Perelomova, N.V., Strizhevskaya, F.N., Chkalova, V.V., and Shaskol'skaya, M.P., *Akusticheskie kristally. Spravochnik* (Acoustic Crystals: A Handbook), Shaskol'skaya, M.P., Ed., Moscow: Nauka, 1982.

Translated by O. Tsarev